Histological and immunohistochemical characterization of feline hepatic lipidosis

Gelens, T.

Three month research internship June-August 2013
Supervisor: Baukje Schotanus and Chiara Valtolina
Date: 4/11/2014
Student #: 3382257
Utrecht University, Faculty of Veterinary Medicine

Table of contents.

Abstract.

Feline hepatic lipidosis is an acute critical syndrome that can result into mortality. Classically this condition is considered to involve merely simple steatosis and not progress into liver failure. During histological evaluation some features of steatitis appear to be present. In human medicine there is a condition called non alcoholic fatty liver disease(NAFLD) involving steatosis, steatitis and cirrhosis, to which feline lipidosis may exhibit similarities. To further investigate feline lipidosis we performed immunohistochemistry on samples that have been histologically graded by the NAS-score, used for evaluation and staging of NAFLD.

Fifteen archival samples of cat liver have been included in this study, of which twelve feline lipidosis samples and three healthy control animals. All feline lipidosis samples have been scored for steatosis, ballooning, inflammation, fibrosis and oval cells resulting in a NAS-score. Samples have been evaluated by immunohistochemical staining for regeneration of hepatocytes or liver progenitor cells(LPC) (Ki67, K19), inflammatory reaction with macrophages and lymphocytes (MAC387, CD3), hepatic stellate cells(HSC) and fibrosis (αSMA, Sirius red).

Feline lipidosis samples show little to no hepatocyte regeneration, little LPC activation and decreased numbers of macrophages and lymphocytes. In all feline lipidosis samples HSC are increased and early fibrosis is present.

Introduction.

Hepatic lipidosis (HL) is a syndrome that commonly develops in cats that become anorectic secondary to an underlying disease (secondary lipidosis) or secondary to diet changes or periods of stress (primary lipidosis). During a period of anorexia, causing a catabolic state, widespread peripheral lipolysis occurs. This results in mobilization of free fatty acid that accumulates in the liver in forms of trygliceride[1]. The accumulation of trygliceride in the hepatocytes is defined lipidosis or steatosis. Although predisposing factors remain incompletely understood, it is clear that there is an imbalance between peripheral fat stores mobilized to the liver, hepatic use of fatty acids (FAs) for energy, and hepatic dispersal of triglycerides via formation of very-low density lipoprotein (VLDL). Previous studies have failed to highlight the primary mechanism for triglyceride accumulation in lipidosis but there seems to be an inability of the liver to keep up with the rate of free fatty acid entrance in the liver. Obese (neutered) cats have an increased risk for developing HL.

Clinically patients with hepatic lipidosis present with jaundice, hepatomegaly and gastrointestinal signs, vomiting, diarrhea or constipation. Severe weakness, ventroflexion of the neck and ptyalism may be present. The prognosis for cats with lipidosis is guarded to poor if therapy is not instituted rapidly. With aggressive supportive care, force feeding and fluid therapy, complete recovery rate is >50%.

In human medicine non-alcoholic fatty liver disease (NAFLD) has become the most common liver disease of western countries (20-30% in general population) and is a major cause of liver related morbidity and mortality. Non alcoholic fatty liver disease seems to be closely related to ‘metabolic syndrome’. Metabolic syndrome (MetS) is an association of different underlying disease: atherosclerotic cardiovascular disease, chronic kidney disease and type 2 diabetes mellitus. Insulin resistance and compensatory elevated plasma insulin level, plays a central part in the development of MetS, but obesity has been described as one of the central causative condition[2]. Increased adipose energy storage increases free FA flux towards other tissues and increased triacylglycerol (TAG) storage, inducing insulin resistance. Insulin resistance is defined as a condition in which normal insulin concentrations fail to achieve normal glucose levels in the blood and thus higher insulin concentrations are required for glucose levels to be within reference.

Adipose tissue produces several inflammatory adipocytokines (TNF-α, IL-6) which have pro inflammatory effects and have a negative effect on blood pressure (hypertension)[3].
Steatosis alone is considered a relative benign disease but 30-40% of patients with NAFLD progress in time, to advanced fibrosis or cirrhosis.

Clinicopathologically NAFLD ranges from simple steatosis to chronic steatohepatitis(NASH). Macroscopic and histological examination is performed with H&E staining and Masson's trichrome. Simple steatosis is characterised by > 5% fat accumulation in hepatocytes, when > 50% fat accumulates in hepatocytes it is named 'Fatty liver'.

Steatohepatitis is characterised by signs of hepatocellular injury including ballooning, apoptosis/necrosis, giant mitochondria and mallory's hyaline (intra cytoplasmic bodies) as well as presence of inflammation and fibrosis (perisinusoidal, pericellular). Ballooning is an irreversible state announcing cell death. Ballooning is characterized by hepatocytes with a central nucleus, surrounded by a white foamy cytoplasm. Distinction with macrovesicular steatosis can be made by evaluating the position of the nucleus which is eccentric during lipidosis.

Lipidosis in human medicine is classified according to the NAFLD activity score (NAS) system. NAS provides a composite score based on degree of steatosis (0-3), lobular inflammation (0-3), hepatocyte ballooning (0-2), with an additional score for fibrosis. A total score < 3 indicates NASH is unlikely, a score ≥ 5 is suggestive of NASH [4].

Reports on histological examination of hepatic lipidosis in cats are rare. In 1993 Center et al described histological and electron microscopical alterations in cats with HL. Abnormalities described consisted of displacement of cell organelles to the cell periphery. The number of vacuoles filled with lipids varied per cat and some cats had a mixture in vacuole size. As a comparison, in human medicine zonal distribution of hepatocyte vacuolation is variable as well. Generally zone 3 steatosis predominates in adult NAFLD and steatohepatitis, zone 1 steatosis predominates in pediatric NAFLD and steroid induced hepatopathy but distribution may also be diffuse (panacinar) or azonal (random, non uniform)[4,5].The endoplasmatic reticulum had dilated areas and mitochondria were decreased in number and disfigured. The peroxisomes were sparse compared to healthy cats. Also the number of observed bile canaliculi were severely decreased. There was not a particular distribution of histological abnormalities in the liver. No signs of inflammation or fibrosis have been described. Based on this report HL in cats resembles human simple steatosis more than NAFLD/NASH[6].

Feline HL shows some similarities in the pathogenesis to human NAFLD. On histological level progression to inflammation and fibrosis is demonstrated in human NAFLD, but this has not been demonstrated in the limited literature available on feline HL.

Our hypothesis is that feline steatosis can progress to steatohepatitis; the hypothesis will be confirmed by findings signs of inflammation, regeneration and fibrosis with the aid of immunohistochemistry

Background.

To better understand the process and the major players in liver regeneration and fibrosis we will initially give some background informations with the aim to elucidate those important processes.

The liver is known for its remarkable regenerative capacity. Surgically remove 70% of the liver mass from rats or mice and within five to seven days after surgery the liver has restored a mass to the equivalent of the original liver. The main cells contributing to the regenerative response are mature hepatocytes and other resident hepatic cells, whereas in other organs such as small intestine or skin, the cells contributing to regeneration are selective subpopulations of stem cells[7]. In rats DNA replication in hepatocytes starts approximately 14 hours after partial hepatectomy and reaches its peak at 24 hours; for mice this peak is later, between 30 and 60 hours[8,9]. Hepatocytes are sometimes considered functional stem cells of the liver for they can all devide at least once. Overturf et al showed a fraction of adult mice hepatocytes can duplicate at least 69 times during serial transplantations[10].

Liver progenitor cells (LPCs) are located in the interlobular bile ducts and canals of Hering. These LPCs have stem-cell-like potential and are a small subpopulation of the ductular cells. These cells invade the parechyma, either as loosely cohesive groups or as ductules or ductular reaction. When hepatocytes are not able to proliferate or not proliferate at a sufficient rate, LPCs are activated. LPC proliferation and differentiation into hepatocytes is triggered by numerous growth factors and cytokines such as TGFα and IL-6, released by, inter alia, inflammatory cells. LPCs are closely related to stellate cells[11], macrophages and the extracellular matrix.

In situation of simple steatosis and lipidosis in human affected by NAFLD, it has been demonstrated that the production of reactive oxygen species and other citotoxic mediators are produced by the circulation of free fatty acid and by the accumulation of trygliceride in the hepatocytes[12]. These reactive oxygen species create enough damage to the resident hepatocytes to induce activation of LPCs to compensate for the inhibited replicative capacity of the hepatocytes

Inflammatory cells producing cytokines, play a central role in liver injury and regeneration. In fact during early liver injury, hepatic sinusoids and venules become invaded by polymorphonuclear leukocytes (neutrophils) that are attracted to the damage site by different chemokines and other inflammatory mediators. To contribute to liver damage neutrophils need to migrate into the liver parenchyma. Hepatocytes undergoing apoptosis, attract

neutrophils by releasing chemokines. Neutrophils adhere to the damaged parenchymal cells and produce reactive oxygen species and other cytotoxic mediators to kill the cell[13].

Kupffer cells (KC), resident macrophages of the liver, account for approximately 15% of all liver cells. Kupffer cells are involved in clearance of various substances from the liver and express several receptors for endocytosis. Kupffer cells can incorporate large particles such as bacteria and red blood cells. KC are heterogenous irregularly shaped cells and adhere to the surface of fenestrated sinusoidal endothelial cells. There are at least two different types of KC. In periportal regions there are twofold more KC than in the centrilobular's one. Periportal KC are larger, more phagocytic and posses greater lysosomal enzyme activities than centrilobular KC. KC life span is still unknown, in literature it has been reported that KC can live from several weeks to six months[14]. TNFα and interleukin-6 are known to be critical factors, priming the liver for the regenerative process and Kupffer cellsare one of the major producer of TNFα. TNFα binds to the TNF receptor on hepatocytesleading to the activation and expression of cytokines and mediators that make hepatocytes susceptible to mitogenic stimuli. Stimulated hepatocytes will then move into cell cycle G1 and S phase from G0, becoming activated and able to regenerate[15].

Fibrosis can be defined as the formation of excess fibrous connective tissue in an organ or tissue in a reparative or reactive process is a normal response to acute and chronic injury. Any chronic disturbance of hepatic homeostasis may elicit fibrogenesis. Fibrosis engages a range of cell types and mediators.
Liver fibrosis, differently than lung fibrosis and kidney fibrosis, arises over a relatively long period of time because of the unique regenerative capacity of the liver. When the liver is injured an hypoxia-induced angiogenic response is the first step in the wound healing process. In the normal liver there is an unidirectional oxygen flow through the liver from the hepatic artery and the portal vein to the central vein. Therefore the centrilobular areas are more likely to be subjected to oxygen deprivation than periportal areas. New blood vessels are constituted from pre-existing vessels.

Sinusoidal remodeling is carried out and hepatic stellate cells (pericytes, HSCs) are activated. In normal liver tissue HSC are located in the space of Disse and express markers characteristic of adipocytes(leptin). HSCs once activated, they become myofibroblast-like cells, obtaining contractile, proinflammatory and fibrogenic qualities. Activated HSCs express myogenic markers (αSMA) and migrate to and accumulate at sites of injury. Mediators involved are platelet-derived growth factor(PDGF), vascular endothelial growth factor (VEGF) and vasoactive substances nitric oxide and carbon monoxide[16]. PDGF are mainly produced

by Kupffer cells and are the major mitogens for activated HSCs,furthermore HSCs are the main extra cellular matrix (ECM) producing cells.

Fibrosis, independently from the pathogenesis, predominantly develops in the portal area from which progresses to the rest of the liver. Fibrogenesis is initially characterized by the development of the so called “ductular reaction”. Cells with progenitor features proliferate into duct-like cells , which spread into the liver parenchyma surrounding the portal area. These ductular progenitor cells release chemotactic and anti-apoptotic factors, contributing to myofibroblast accumulation in the portal area, increasing hepatic fibrogenesis.
Activated HSCs express cell adhesion molecules, secrete inflammatory chemokines and modulate lymphocyte activation. A vicious circle is likely to occur with inflammatory and fibrogenic cells stimulating each other[17,18].

Immunostaining.

Tissue samples are embedded in paraffin to maintain the natural shape and structure during long-term storage. Paraffin can be removed with chemical solvents. In this study xylene is used. Fixation of tissue with formalin is based on (semi) reversible protein cross linking and dehydration, covering epitopes used in IHC. Therefore tissue is rehydrated in baths with different ethanol concentrates and antigen retrieval steps need to be performed to retrieve epitopes used in IHC[19].

Heat-induced antigen retrieval is a simple method to retrieve immunohistochemistry epitopes. Paraffin embedded tissue is placed in a water bath (95-100 °C) with buffered water solutions for 30-60 min. Thereafter the slides are cooled down by placing the container outside the bath at room temperature. The antigen retrieval leads to renaturation of the protein structure or at least partial restoration of the structure approaching its native condition[19].

Enzyme induced antigen retrieval can be achieved by ready to use enzymatic digestion solutions. Protein kinase K is a proteolytic enzyme solution diluted in Tris-HCl and sodium azide buffer (pH 7,5). Protein kinase K is used for proteolytic digestion of formalin fixed, paraffin embedded tissue sections which improves accessibility of epitopes and probes that have been masked during fixation. Presumably the enzymes cleave the cross-links between proteins, allowing the protein to return to its normal conformation[19].

Commonly enzymes found in cells are also used as reagents in immunohistochemical visualisation procedures. Reagents involved are endogenous biotin, peroxidases and phosphatases. These endogenous enzymes can interfere during antigen detection, creating false positive results by generating unwanted signals. For IHC staining in this study peroxidase activity is found to be most relevant. Endogenous peroxidase activity can be inhibited by several methods. Methods used in this study are 1% H2O2 in methanol and Dako ready to use peroxidase block which both eliminate endogenous peroxidase activity[19,20].

IHC antibodies bind to specific tissue sites but may also bind to non specific sites (partially or weakly). These sites are similar to binding sites of the antigen and cause high background staining. High background staining can camouflage the target antigen. To reduce background staining the tissue is incubated with a blocking buffer that blocks the reactive sites. In this study 10 percent normal goat serum is used to achieve this.

Target antigen is detected with antibodies. Antibodies bind to tissue antigen. Antibody incubation time and temperature, as well as antibody titer and dilution can be changed to optimize the staining. In optimal staining the target antigen is stained specifically and there is minimal interference from background staining. The optimum antibody titer is the highest dilution that results in maximum specific staining. The optimum antibody titer is determined by the inherent affinity of an antibody. With a constant antibody titer an antibody with high affinity is more likely to give intensified staining and react faster than an antibody with low affinity. Antibody dilution contributes to the quality of staining. The dilution gives a peak staining intensity and also the presence of minimal background staining, thus maximum signal-to-noise ratios can be achieved with the right dilution. Incubation time is often fixed during determination of the optimal antibody dilution. The higher the antibody titer, the shorter the incubation time required. Incubation time can vary from 10 min to 24 hours. In this study we use one hour incubation time or incubation overnight. The incubation temperature is important as well. At 37°C the antibody-antigen reaction reaches equilibrium most rapidly. During longer incubation times, lower temperatures are used. In this study incubation overnight is at 4°C while incubation for one hour is at room temperature. During long incubation time it is important to place the slides in a humid environment so they will not dry out.

To visualize antibody secondary antibodies or labelled first antibodies are required. Different types of methods exist, like avidin-biotin complex, peroxidase anti-peroxidase complex and the two step polymer method. In this study a two-step staining technique from DAKO has been used. It is based on an HRP labelled polymer which is conjugated with secondary antibodies and binds to the primary antibody. To visualize the secondary antibodies 3,3-diaminobenzidine (DAB), a liquid chromogen, is used. This is a two component system with a solution containing HRP substrate buffer in H2O2, and a solution with the DAB chromogen substrate. Detection of peroxidase is based on conversion of diaminobenzidine (this study) or other aromatic phenols and amines into water-insoluble pigments in the presence of H2O2. Finally this results in a brown colouration of the secondary antibodies of the target tissue and/or cells[19,20].

The hepatic cytoskeleton consists of microtubules, actin and intermediate filaments. Keratins are the most important family of intermediate filaments and are mainly expressed in epithelial cells and skin adnexa. Keratins can be subdivided into subgroups by unique amino acid signatures. Adult hepatocytes express Keratin8(K8) and Keratin18(K18) which are keratins of single layered and glandular epithelia. K8/K18 has not been included in this study. Keratin19(K19) is mainly expressed in bile ducts and it is considered a marker of liver

progenitor cells (LPCs). LPCs are considered stem cells and under the influence of different cytokines and of their niche ,have the ability to differentiate into hepatocytes or cholangiocytes[21,22]. K19 was used in this study to visualize ductular reactions and activation of LPCs.

Hepatocyte proliferation activity can be determined by Ki67 staining. Ki67 is an antibody based on the Ki67 protein antigen located in the nucleus during all cell cycle phases, except during the resting phase. In healthy liver tissue there are always few replicating hepatocytes present and during liver injury the amount of replicating hepatocytes increases. Ki67 is therefore a widely used marker of cell proliferation and is an excellent marker to determine the proliferation activity in a given cell population. Until today the function of the Ki67 protein during the cell cycle is unknown[23]. Ki67 is also expressed by immune cells like neutrophils. Ki67 in this study is used to measure the amount of proliferating hepatocytes to assess the regenerative activity of these mature liver cells.

Alpha-smooth muscle actin (α-SMA) is the most specific and most widely accepted antigen to stain activated HSCs with IHC[24]. α-SMA is an important marker of ECM producing cells and indicate potential ECM production. During liver injury there is progression to fibrosis, studied with αSMA and Sirius Red staining. αSMA stains myofibroblasts, in healthy liver tissue only present around bloodvessels and other endothelial cells. In diseased livers myofibroblasts migrate towards injured cells, and mainly reside in and around the sinusoids.

Sirius Red stains collagen types I, II, III and VI. Collagen is the major fibrous protein in extracellular matrix and connective tissue and visualises early and chronic fibrosis[25,26].

Two markers for inflammatory responses have been used. CD3 is a marker of lymphocytes. MAC387 is a marker of macrophages. During liver injury inflammatory responses can be expected. Cells involved can be macrophages, lymphocytes and polymorphonuclear lymphocytes (PMLs). MAC387 stains macrophages and CD3 stains lymphocytes.

Material and methods.

The project was approved by the responsible ethical committees for the use of client owned animals according to Dutch legislation. Liver biopsies of cats diagnosed with lipidosis were selected from the archives of the Department of Pathobiology of the Faculty of Veterinary Medicine at the University of Utrecht.

Fifteen biopsy samples of cats' liver have been included in this study and divided in three groups. Group 1 consists of six true cut liver biopsies obtained for diagnostic purposes, from client owned cat affected with liver lipidosis, . Groups 2 and 3 contain three wedge biopsies, each obtained post mortem from deceased cats during post-mortem examination. Biopsies from affected animals have been selected after histological examination and NAS scoring performed by a boarded specialist in veterinary pathology. anamnesis of the animals and histological (NAS) scores have been listed in tables 1 and 2 respectively. Group 1 consists of six true cut biopsies with high NAS score. Group 2 contains three wedge biopsies with high NAS scores. Group 3 consists of three wedge biopsies with low or intermediate NAS scores. Each specimen was fixed in formalin and embedded in paraffin. Sections paraffin were cut and mounted on a slide.

Table 1. History and signalment

ID	Signalment	History
Group 1		
P9609378	European shorthair, castrated male, 6Y old	Dysorexia, weight loss, lethargic, vomiting, anemia(Ht 0,09). Started on dexamethason (IHA?) Euthanised few days later.
P0102523	Unknown	Unknown
P0110084	Unknown	Unknown
P0309444	European shorthair, castrated female, 10Y old	Since 10 days lethargic, anorexia, adipsia. On presentation cat was icteric, nauseated, dehydrated. Died after sedation for liver biopsies.
P0312037	European shorthair, castrated female, 5Y old	Since one week anorexic, lethargic. Vomiting upon force feeding. On presentation the cat had lost weight, was icteric, dehydrated and painful on abdominal palpation. An oesophageal feeding tube was placed. Diagnosis: Lymphocytic enteritis. Discharged with feeding tube and anti-emetics. One week later she ate on her own again.
P0410061	European	Dysorexia since few weeks, mass in ventral neck. Mass was removed.

	shorthair, castrated male, 13Y old	Feeding tube was placed. Cat was discharged with feeding tube and medication. Few days later re-admitted with nystagmus and disorientation. Cat was euthanized.
Group 2		
J310113000502	European shorthair, female, 5-6 months old	Diarrhea for unknown period of time, general malaise, enlarged intestines on palpation and CBC shows severe inflammation. Pathology: mild acute multifocal necrosuppurative hepatitis.
J310082704402	Norwegian Forest Cat, 5Y old	Red urine since one week, loss of appetite (lost 1,5 kg), jaundice with enlarged liver. Other cat in the house shows same symptoms. Pathology: extensive lipidosis.
J311051000202	Crossbreed, female, 5Y old	Anorectic for two weeks, vomiting, adipsia, jaundice, increased liver values, no improvement despite aggressive therapy with fluids, feeding tube and medication. Pathology: severe hepatic lipidosis with severe bile stasis
Group 3		
J311061503102	European shorthair, 2,5Y old	Laboratory animal with cachexia, anorexia, jaundice, dehydration, vomiting. Pathology: mild diffuse lipidosis with cholestasis, possibly feline infectious peritonitis (FIP)
J311121504002	Crossbreed, 8 months old.	Found dead in the garden. Pathology: Cause of death most likely trauma, severe hepatocellular lipidosis
J311031104902	10 months old	Died suddenly, showed pica and only ate canned food prior to death. Pathology: cholangiohepatitis and lipidosis.
Control group		
Rafael	6Y castrated male,	Other than dental cleaning no striking features. Vaccinations and deworming according to protocol. Bloodwork (2011) within reference.
Mazzel	9Y male	Other than otitis(twice), conjunctivitis(once) and extensive dental treatment including two extractions no striking features.
Ozzy	9Y male	Other than dental cleaning and few times deviating coagulation values (probably due to laboratory artefacts) no striking features.

Table 2. Histological scoring

ID	Steatosis	Ballooning	Lobular inflammation	Portal inflammation	Fibrosis	Oval cells	NAS	Relative Size (µ)
Group 1								
P9609378	3	2	1(N)	0	0	0	6	43430
P0102523	3	2	1(N)	0	0	0	6	10468

P0110084	3	1	1(N,L)	0	0	0	5	35879
P0309444	3	1	2(N)	0	0	0	6	23135
P0312037	3	2	2	0	0	0	7	16316
P0410061	3	1	2(N,L)	0	1	0	6	14517
Group 2								
J310113000502	2	1	2(N,L)	0	0	0	5	55619
J310082704402	3	2	0	0	0	0	5	55569
J311051000202	3	1	1(N,L)	0	0	0	5	55687
Group 3								
J311061503102	1	0	0	0	0	0	1	44794
J311121504002	2	0	1(L,P)	0	0	0	3	55212
J311031104902	3	0	1(L,P,N)	1	0	0	4	53365
Control group								
Rafael	-	-	-	-	-	-	-	31655
Mazzel	-	-	-	-	-	-	-	24599
Ozzy	-	-	-	-	-	-	-	27796

During IHC staining the following steps are performed. Sections are deparaffinised and rehydrated in a series of Xylene:2x5 min., Alc. 96%, Alc. 80%, Alc. 70%, Alc. 60%, MQ, each step 5 minutes. Antigen retrieval and endogenous peroxidase block was performed as specified in table 3. Each slide is incubated in normal goat serum (10%) to reduce background staining. Antibodies and concentrations used are specified in table 3. Slides are incubated in envision goat anti mouse or anti rabbit, depending on the type of antibody used, for 45 min at room temperature. To visualize immune reaction sections were stained in DAB. Slides are washed in milliQ and counterstained with haematoxylin QS- Dako in a 1:1 dilution with milliQ for 10 seconds. Slides are washed in running tap water for 10 min. Slides are dehydrated and fixated with a series of ethanol dilutions and the last two steps are xylene, each step 3 minutes. Slides were covered with vectamount for good preservation. In the appendix the protocols have been included.

Table 3. Overview immunohistochemistry stainings

Staining	Antibody	Antibody concentration	Antigen retrieval	Endogenous peroxidase block	Washing buffer
K19	K19 mouse	1:100	Proteinase-K (Dako)	Dual endogenous enzyme block (Dako)	TBS(/T)
Ki67	Ki67 MIB-1 mouse	1:30	Hot citrate buffer pH 6.0	Dual endogenous enzyme block (Dako)	PBS(/T)
αSMA	αSMA mouse	1:200/1:50	-	1% H2O2 in methanol	PBS(/T)
Sirius Red	Sirius Red F3B	0.5g/500ml	-	-	-
MAC387	MAC387 mouse	1:1000	Proteinase-K (Dako)	Dual endogenous enzyme block (Dako)	PBS(/T)
CD3	CD3 rabbit	Wedge/FNAB 1:200/1:400	Hot citrate buffer pH 6.0	Dual endogenous enzyme block (Dako)	PBS(/T)

To perform a cell count on MAC387 ImageJ, a java based image processing program from the National Institutes of Health, has been used. With a photo microscope pictures have been taken at 4x objective. First the outline of the tissue on the picture has to be selected and large stromal areas have to be excluded. The outside of the outline is cleared to allow the program to count the true surface area. The second step is enhancing the contrast of the positively stained cells relative to the other cells with the color deconvolution plugin. This plugin automatically converts the picture to an 8 bit image. As this is completed the threshold needs to be adjusted so that only positively stained macrophages remain. This can be verified by looking at the macrophages in the original image. After this a black and white image remains. If there are multiple macrophages attached to each other they can be

separated by using the watershed option in the binary section. Select the option analyze particles and a cell count is performed by ImageJ. To check accuracy positive cells in three of fifteen samples, varying from low to high numbers of positive cells, have been counted by hand and compared to the cell count results. The numbers obtained deviated by one to five cells and this is assessed as an acceptable divergence. The cell count for Ki67 and CD3 has been done by hand because other cells than respectively hepatocytes or lymphocytes stain positive as well. Cells can only be differentiated by looking at a high magnification. Therefore on each slide five fields at a 40X objective have been observed for positive stained hepatocytes and lymphocytes.

Original scores have been adapted to the area of interest. For K19, parenchymal cells are most important and periportal is important as well since these areas contain possible ductular reaction. The final score consists of the initial periportal score and parenchymal score multiplied by two, added together. Activated stellate cells migrate towards injured tissue, which is expected to be mostly parenchymal with some periportal activity. Therefore parenchymal and periportal cells positive for αSMA are most important and the final score is the periportal score and the parenchymal score multiplied by two added together. For Sirius Red all areas have been included at the same rate because collagen deposition during liver injury is possible throughout the tissue.

Results.

For all animals the number of positive stained cells was very variable, as well as the area where they were found. Therefore a distinction has been made within initial scoring, for portal, periportal and parenchymal positivity.

Liver regeneration is studied with K19 staining for LPCs activation and Ki67 staining, for hepatocytes replication. To be able to assess if those staining were working in cats, we used biopsies of cats small intestines as positive control; K19 and ki67 stained nicely the fast replicating enterocytes in cats intestines. In healthy control animals we were expecting positive bile ducts in the portal areas, no ductular reaction and no positivity to any of the stained used outside the portal areas. Looking at the results in table 4 it is possible to notice a large individual variation for k19 and ki67. There appears to be no correlation between k19 and ki67. For group 1 and 2 the ballooning score of the pathologist appears to correlate to the presence of ki67 positivity. In group three however this finding is not present and for the control group there is no ballooning score available. worth of mention is that samples with high NAS score appear to contain less K19 or Ki67 positive cells.

Table 3. Correlation between NAS scoring system, ballooning , oval cells and K19 or Ki67

ID	NAS	Ballooning	Oval Cell	K19	Ki67 cells/five 40x fields
Group 1					
P9609378	6	2	0	1	4
P0102523	6	2	0	6	1
P0110084	5	1	0	2	0
P0309444	6	1	0	1	0
P0312037	7	2	0	5	1
P0410061	6	1	0	0	0
Group 2					
J310113000502	5	1	0	4	0
J310082704402	5	2	0	9	15
J311051000202	5	1	0	4	3
Group 3					
J311061503102	1	0	0	6	7
J311121504002	3	0	0	5	1
J311031104902	4	0	0	9	32
Control group					
Rafael	-	-	-	4	3
Mazzel	-	-	-	4	5
Ozzy	-	-	-	4	11

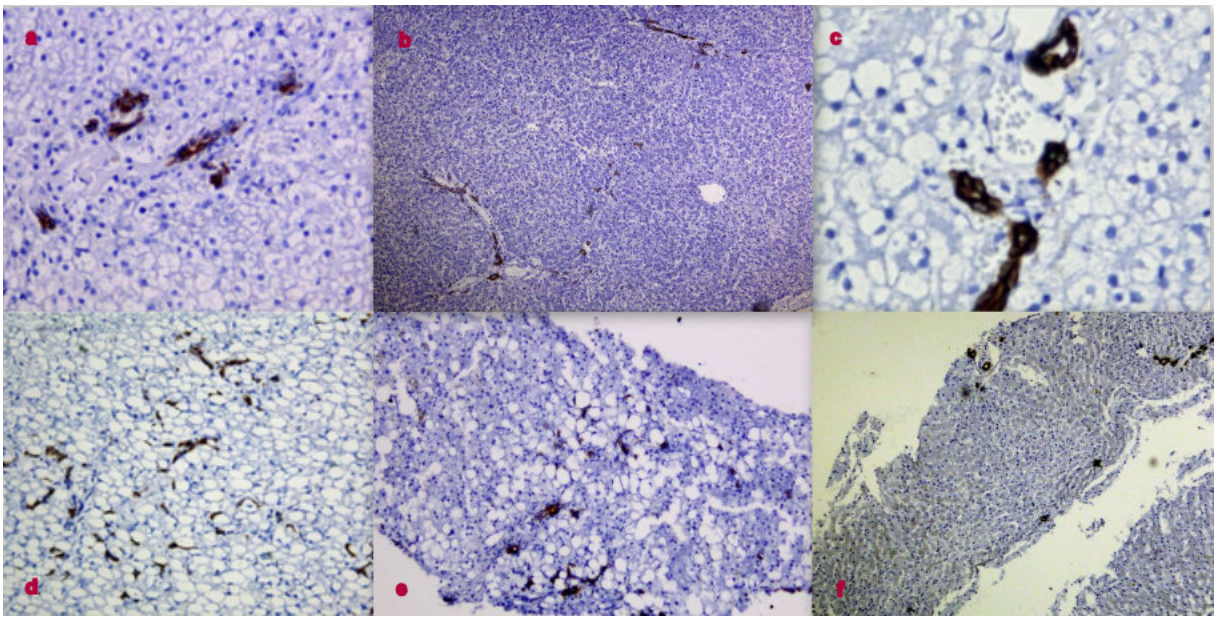

K19. Photo a. True cut biopsy from control with increased LPC activation, loose cells in the parenchyma. Photo b. Wedge biopsy of low NAS score, with increased peri portal K19 expression. Photo c. Control animal(Mazzel) with increased LPC activation in the portal area. Photo d. Wedge biopsy of high NAS score with ductular reaction. Photo e. True cut biopsy with increased periportal and parenchymal activation of LPC's Photo f. True cut biopsy from control with some portal and periportal activation of LPC's.

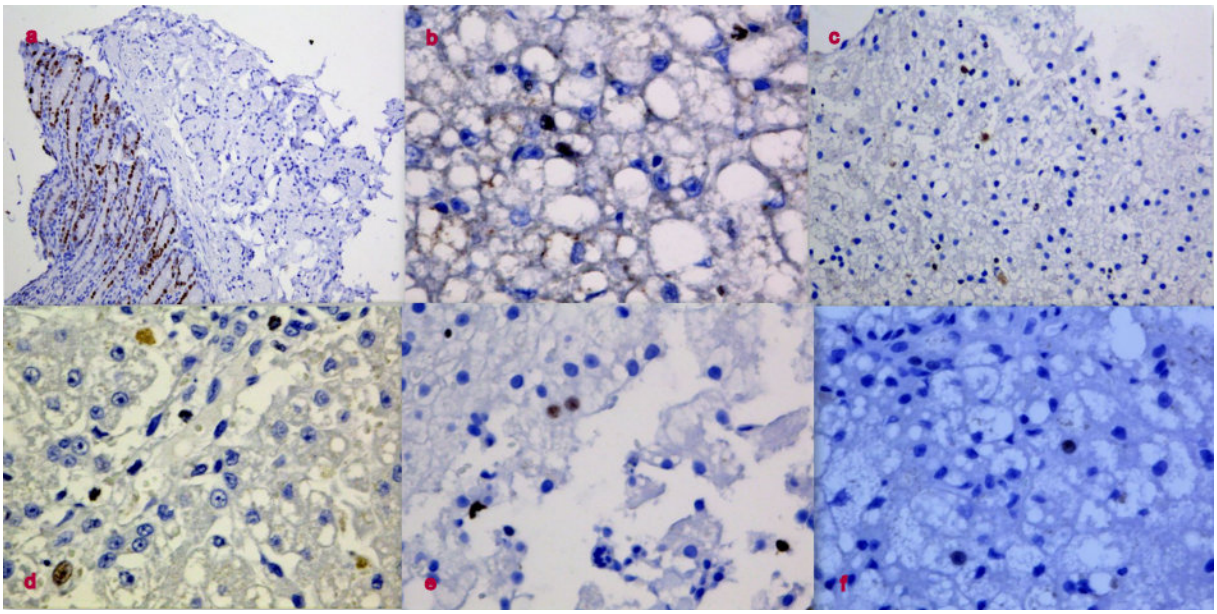

Ki67. Photo a. Positive control duodenum of a cat, Ki67 positive cells in the crypts. Photo b. Wedge biopsy with Ki67 positive PML's, no hepatocytes. Photo c. True cut biopsy from control animal with positive hepatocytes and inflammatory cells. Photo d. Wedge biopsy with Ki67 positive hepatocyte just outside the portal area. Photo e. True cut biopsy from control animal containing two positive hepatocytes in the center. Photo f. True cut biopsy with high NAS score containing a positive hepatocyte.

Liver fibrosis has been evaluated with αSMA and Sirius Red staining. In healthy liver tissue Sirius Red positivity is present in the portal area, since collagen is normally present in the basement membranes of bile ducts and vessels. αSMA positivity in healthy liver tissue is present around blood vessels and bile ducts. For this staining we used kidney and small intestine biopsies as positive control. There appears to be no correlation between presence of increased αSMA positivity and increased Sirius Red positivity. The pathology scores for fibrosis do not seem to relate to the results of the stainings.

However it appears that an higher positivity score for αSMA and Sirius Red is related to a high NAS score , even if the result is not statistically significant.

Table 5. Overview fibrosis markers

ID	NAS	fibrosis	αSMA	Sirius Red
Group 1				
P9609378	6	0	7	4
P0102523	6	0	6	8
P0110084	5	0	3	4
P0309444	6	0	2	4
P0312037	7	0	9	8
P0410061	6	1	1	8
Group 2				
J310113000502	5	0	10	2
J310082704402	5	0	11	6
J311051000202	5	0	12	3
Group 3				
J311061503102	1	0	8	3
J311121504002	3	0	6	4
J311031104902	4	0	12	5
Control group				
Rafael	-	-	2	6
Mazzel	-	-	3	2
Ozzy	-	-	1	2

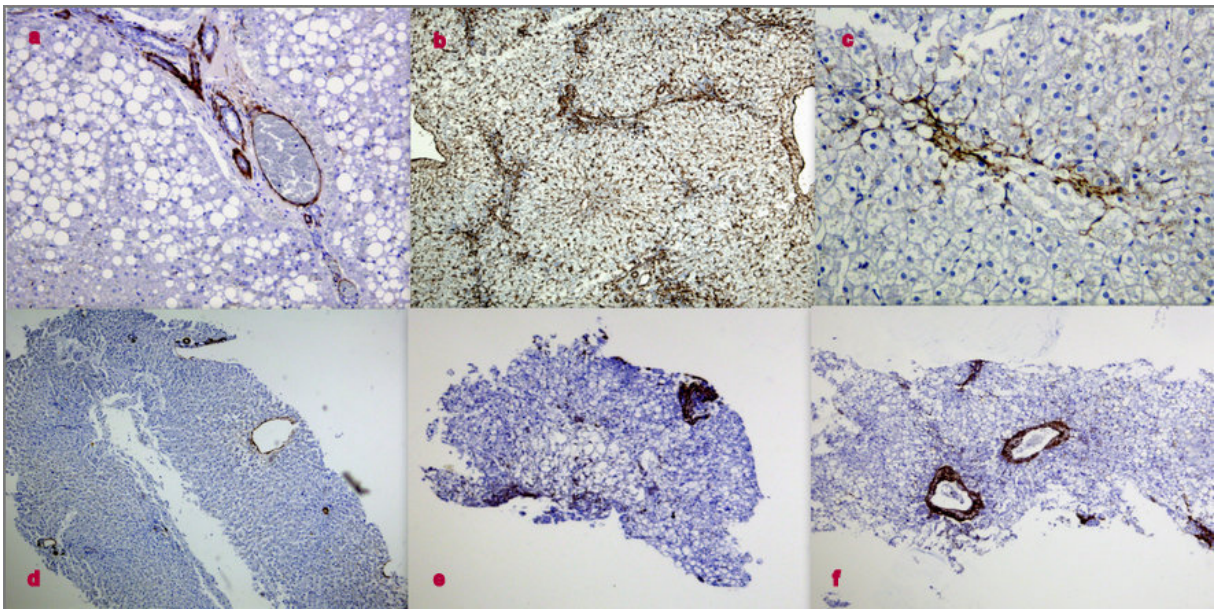

αSMA. Photo a. Wedge biopsy with low NAS score with increased αSMA positivity in the portal area. Photo b. Massive stellate cell activation in cholangio hepatitis wedge biopsy with high NAS score. Photo c. True cut biopsy from control animal containing increased periportal stellate cell activation. Photo d. Control sample with little αSMA activity. Photo e. True cut biopsy with high NAS score with increased Stellate cell activity in the portal, periportal and parenchymal area. Photo f. True cut biopsy with high NAS score with portal and periportal activation of stellate cells.

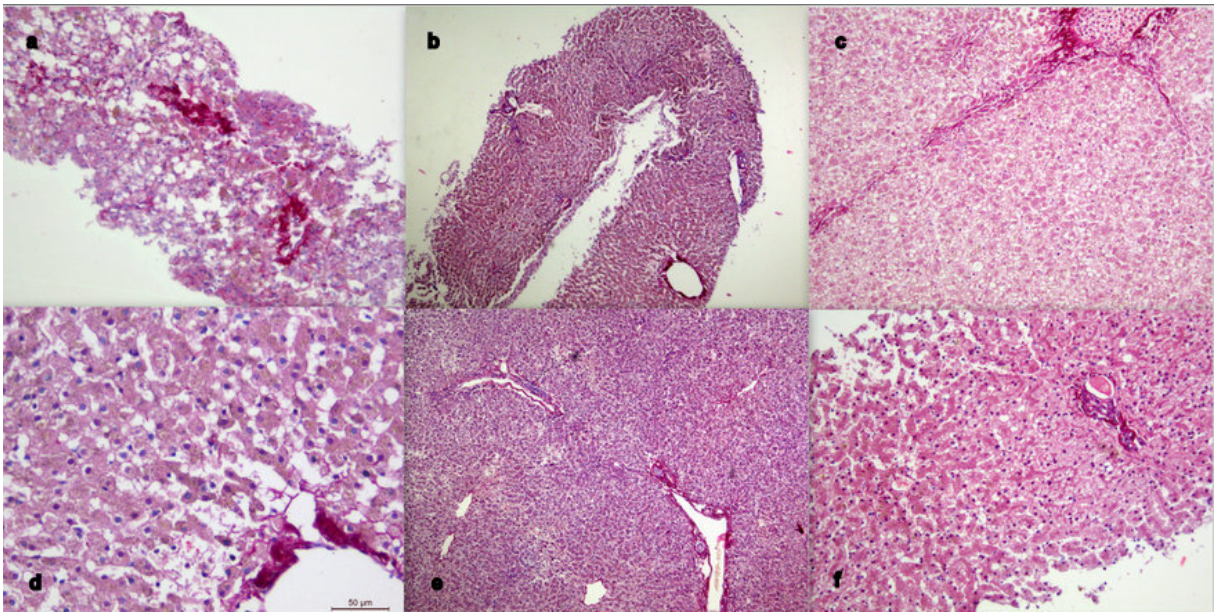

Sirius Red. Photo a. True cut biopsy with high NAS score with a lot of collagen deposition in portal, periportal and parenchymal areas. Photo b. True cut biopsy from conrol animal with little collagen depositions. Photo c. Wedge biopsy with high NAS score from animal with acute fulminant hepatitis containing portal bridging. Photo d. Control animal with minimal increased portal and periportal collagen depositions. Photo e. Wedge biopsy with low NAS score containing little Sirius Red positivity. Photo f. Control biopsy with a small increase of collagen deposition in the portal area.

For the MAC387 and CD3 stainings we used cat's lung tissue and a biopsy of lymphocytic cholangitis as positive control. During lymphocytic cholangitis there are aggregates of lymphocytes in the portal tracts and around bile ducts. Comparing groups, MAC 387 has notable distribution differences through the slide. In all biopsies macrophages are present in the parenchyma. Samples in group 1 showed little macrophage presence through the entire slide. In groups 2 and 3 the macrophages could be found in all parts of the tissue although the majority of the MAC387 positive cells are in and around the portal areas. Cell count with ImageJ reveals a decreased number of macrophages in group 1 as compared to the other groups. CD3 cell count by hand also reveals a decrease in number of lymphocytes in group 1. The results do not always correlate to the pathology scores. There are slides that scored "0" for inflammation by the pathologist, in which we noticed an increased numbers of positive cells; in contrary there are slides with little to zero positive stained cells but scored by the pathologist with a "1" or "2" score.

Table 6. Overview inflammation scores.

ID	NAS	Lobular inflammation	Portal Inflammation	MAC387 Cell count	MAC387 cells/surface biopsy	CD3 cells/five 40X fields
Group 1						
P9609378	6	1(N)	0	112	0,002579	0
P0102523	6	1(N)	0	17	0,001624	3
P0110084	5	1(N,L)	0	28	0,00076	0
P0309444	6	2(N)	0	66	0,0029	0
P0312037	7	2	0	21	0,001287	3
P0410061	6	2(N,L)	0	56	0,003858	0
Group 2						
J310113000502	5	2(N,L)	0	332	0,005969	2
J310082704402	5	0	0	142	0,002555	15
J311051000202	5	1(N,L)	0	224	0,004022	35 Mainly parenchymal
Group 3						
J311061503102	1	0	0	182	0,004063	7
J311121504002	3	1(L,P)	0	175	0,003175	7
J311031104902	4	1(L,P,N)	1	2287	0,042687	28 Mainly portal
Control group						
Rafael	-	-	-	344	0,010867	9
Mazzel	-	-	-	118	0,004797	4
Ozzy	-	-	-	83	0,002986	8

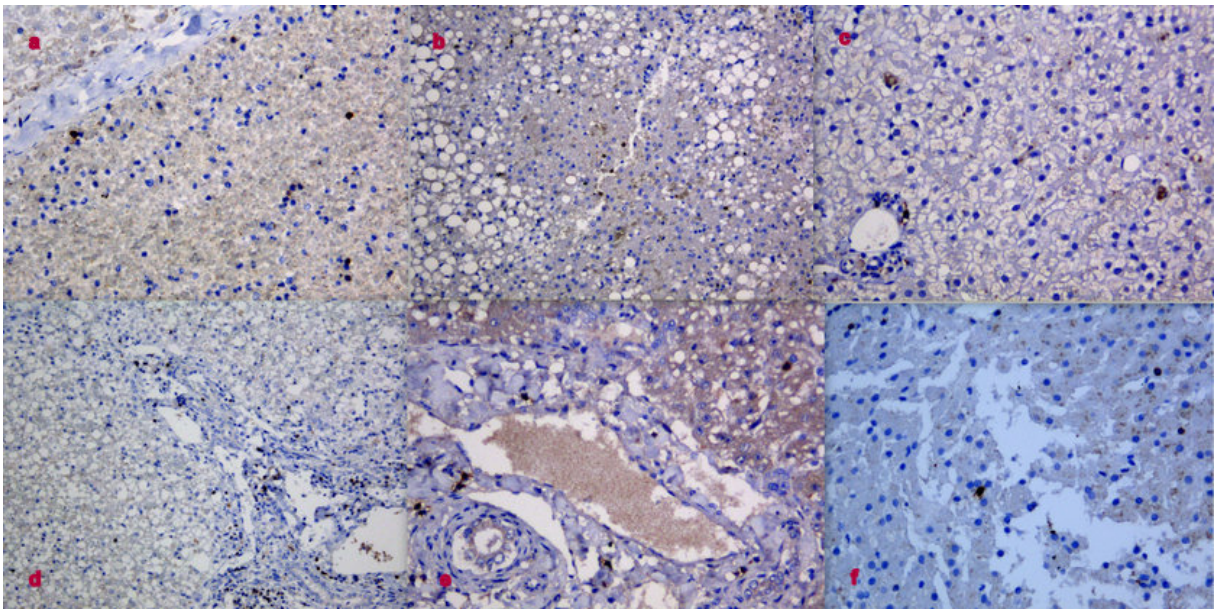

CD3. Photo a. CD3 positive lymphocytes in portal, periportal and parenchymal area in acute fulminant hepatitis. Photo b. Low NAS score wedge biopsy with CD3 positive lymphocytes. Photo c. Control animal with positive lymphocytes in and around the portal area. Photo d. Cholangio hepatitis containing many lymphocytes in the portal area. Photo e. Wedge biopsy with low NAS score containing lymphocytes in and around the portal area. Photo f. Control animal with lymphocytes in the parenchymal area.

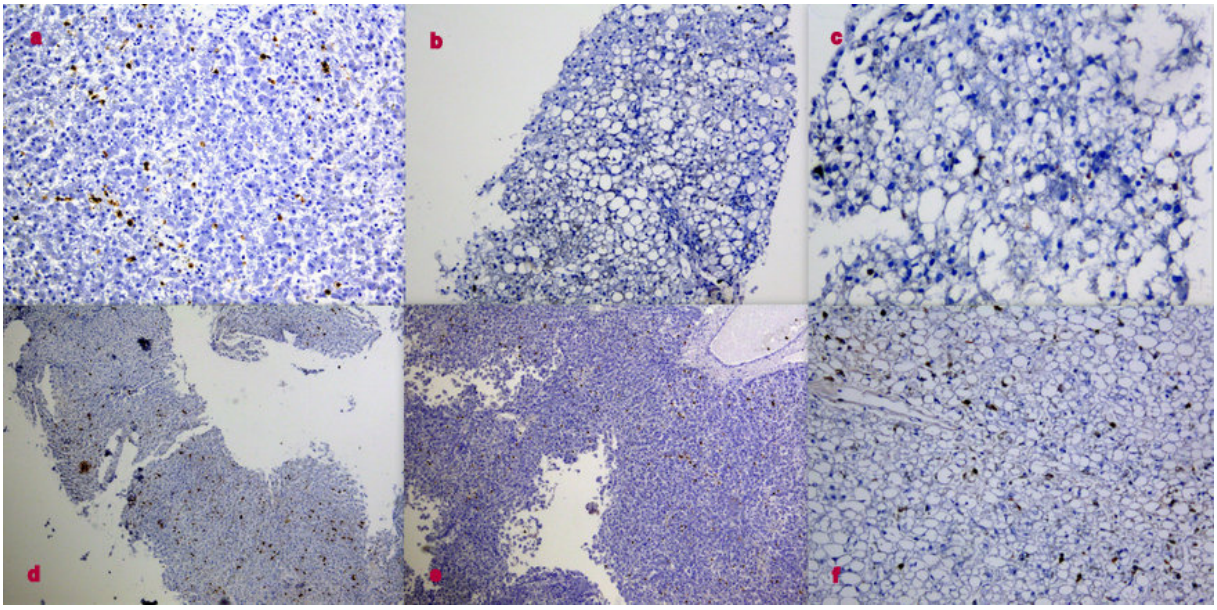

MAC387. Photo a. Wedge biopsy with low NAS score containing numerous macrophages in the portal and periportal area and the parenchyma. Photo b. High NAS score true cut biopsy containing very little macrophages. Photo c. High NAS score true cut biopsy containing some macrophages in the parenchyma. Photo d. Control animal biopsy containing numerous macrophages in the portal and periportal area and in the parenchyma. Photo e. Same biopsy as photo a., macrophages are present in the portal, periportal and parenchymal area. Photo f. Wedge biopsy with high NAS score containing macrophages in periportal, portal and parenchymal areas.

In table 7. scores for K19, MAC, CD3, αSMA and the ballooning score given by the pathologist have been included. There seems to be no relationship between ballooning and the number of inflammatory cells present. There is also no visible correlation between K19 activation and the number of inflammatory cells present.
Samples with low Ki67 expression contain low amounts of CD3 positive cells. Samples with low MAC387 expression contain low amounts of CD3 positive cells. Two samples show a different trend, as earlier described : the biopsies from cat with acute fulminant hepatic failure and lymphocytic cholangiohepatitis.

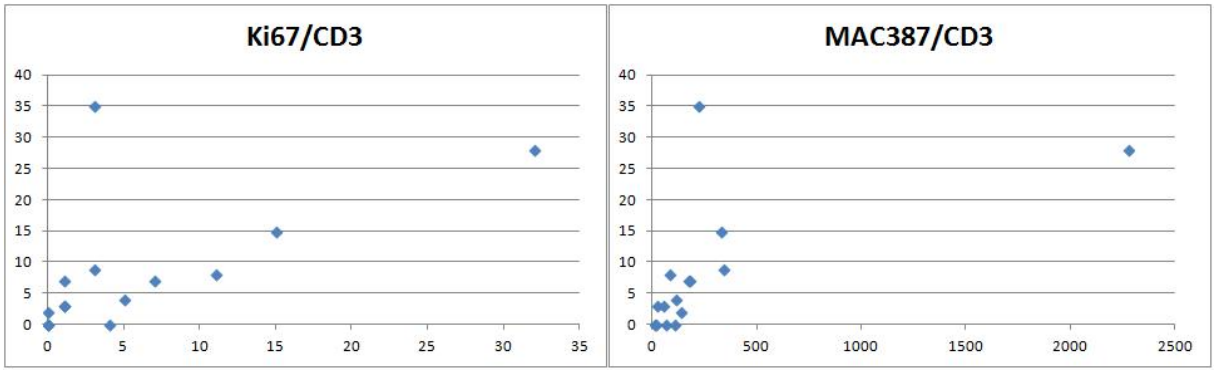

Graphics 1 and 2. 1 shows CD3 score on X-axis and Ki67 on Y-axis. There appears to be a correlation between regeneration and presence of lymphocytes. 2. Shows MAC387 on X-axis and CD3 on Y-axis. There appears to be a correlation between presence of macrophages and lymphocytes.

Table 7. Overview scores for inflammation, regeneration and myofibroblast activity related to ballooning.

ID	Ki67 cells/five 40x fields	K19	αSMA	MAC387 Cell count	CD3 cells/five 40X fields	Ballooning
Group 1						
P9609378	4	1	7	112	0	2
P0102523	1	6	6	17	3	2
P0110084	0	2	3	28	0	1
P0309444	0	1	2	66	0	1
P0312037	1	5	9	21	3	2
P0410061	0	0	1	56	0	1
Group 2						
J310113000502	0	4	10	332	2	1
J310082704402	15	9	11	142	15	2
J311051000202	3	4	12	224	35 Mainly parenchymal	1
Group 3						
J311061503102	7	6	8	182	7	0
J311121504002	1	5	6	175	7	0
J311031104902	32	9	12	2287	28 Mainly portal	0
Control group						
Rafael	3	4	2	344	9	-
Mazzel	5	4	3	118	4	-
Ozzy	11	4	1	83	8	-

Discussion.

Lipidosis has been described in literature as an acute critical syndrome that does not progress into liver failure. From an histological point of view its characterization is based on old literature that described feline lipidosis as simple steatosis that lacks of necroinflammatory findings. Evaluation of feline lipidosis biopsies, using the score that has been suggested for classification of NAFLD[5] has highlighted the presence of inflammation, cell ballooning and in one sample of fibrosis. To better evaluate inflammation, regeneration and fibrosis in lipidosis we choose to run immunohistochemistry with different stainings to be able to evaluate all these components in samples with a variable degree of NAS scoring. Group 1 with the highest NAS scores does not show the highest scores for inflammation, regeneration and fibrosis. Group 2, high NAS scores and group 3, intermediate NAS scores, show varying results and the control group scores are higher than expected. All samples show little regenerating hepatocytes or active LPCs and overall there are low amounts of inflammatory cells present which are even lower in more severely affected lipidotic livers. Some fibrosis is present in all samples but there are little active myofibroblasts.

As the degree of steatosis and NAS increases presumably the degree of liver damage increases as described during NAFLD. Hepatocyte regeneration, in cats with lipidosis with high NAS score, appears to have decreased compared to control samples and samples with low NAS scores. Roskams et al 2003 showed obese mice also have impaired hepatocyte regeneration. Once hepatocyte replication is impaired however LPCs are expected to be activated during liver damage. Mice with obesity and lipidosis show activation of oval cells prior to and following a partial hepatectomy[12]. Research by Yang et al 2004 demonstrated a significant increase in H_2O_2 production, toxic reactive oxygen species, by mitochondria from mice with fatty livers compared to healthy controls. Replication of mature hepatocytes is irreversibly impaired and it is accompanied by a substantial amplification of the progenitor cell population[27]. Another study by Sydor et al 2013 showed that mice with mild steatosis, fed a western diet, do not have impaired regenerative capacities of the liver and cell proliferation is significantly enhanced[28]. Conclusion of the study was that mild steatosis induced by western diet lacks of inflammation and lack of all metabolic derangements that characterize NAFLD. Human NAFLD samples show activation of the progenitor cell compartment starting from Brunt fibrosis stage 2, including zone 3 perisinusiodal fibrosis and portal fibrosis[5]. During a study by Katoonizadeh et al 2006, liver regeneration during human acute severe liver impairment showed that with increasing degrees of liver damage also the activation of LPCs increases. A threshold of 50 percent hepatocyte loss was associated with a significant decrease in the proliferative activity of remaining mature hepatocytes, and extensive hepatic

progenitor cell activation. LPC activation is a sign of disease severity and occurs early (within 1 week) in the disease course[29]. Perhaps for cat liver the NAS-score is not correlated to the severity of lipidosis and other staging methods could be more indicative of liver damage and impairment[30]. Another possibility for impaired LPC activation in the samples of this study is the acute course of disease providing little time for the LPC compartment to respond.

We expected all inflammatory cells to be increased during hepatic lipidosis as described during NAFLD by Brunt et al 1999[30]. This increase in inflammatory cells is not present with MAC387 or CD3 positive cells. Macrophages and lymphocytes are not increased but decreased, absent or equivalent to the number of inflammatory cells that are present in control samples. The only exceptions are samples of cats suffering from an acute fulminant hepatic failure and lymphocytic cholangiohepatitis; in those samples a large inflammatory response with marcophages and lymphocytes was seen.
Cell-mediated immunity has been found to play an important part during liver regeneration. Immune responses may regulate or inhibit regeneration. Natural killer cells and natural killer T-cells have been investigated in their role in regeneration during viral infection in mice by Sun and Gao 2004[31]. NK cells comprise approximately 50% of lymphocytes present in the liver. With this study has been demonstrated that liver regeneration is inhibited by activation of innate immunity with increased NK cell and interferon-γ(IFN- γ) activity. The exact mechanism however is still unknown, IFN- γ may induce cell cycle arrest or cell death. Another study by Strick 2008 demonstrated that both natural killer cells and T cells play an important part in regeneration[32]. Feeding a choline-deficient ethionine-supplemented food induces a strong LPC response in healthy mice. Mice without T cells and NK cells perish of acute liver failure and lack an adequate LPC response. Both cell types however are required for a strong LPC response. It is hypothesized that intrahepatic lymphocytic cells support oval stem cell proliferation by secreting cytokines[32]. Low levels of lymphocytes could be an explanation for the severe course of disease and absence of LPC activation.

The finding that feline lipidosis doesn't involve the presence of an increased number of inflammatory cells is contradictory to our expectations. According to the histological NAS scoring of the samples used, inflammation is present in eleven out of twelve samples from affected animals with neutrophils being the more common inflammatory cells seen. During human NAFLD the inflammatory response is correlated to LPC activation[30]. From our results the number of macrophages and lymphocytes also appears to be correlated to the number of LPC's present, both lower than expected.
There are possible explanations for absence of an increased number of inflammatory cells. We have to consider that the cell count performed for MAC387 and CD3 might be an

underestimation in samples with high steatosis score. Since hepatocytes are severely filled with lipids they expand and become two to three times the size of normal hepatocytes. Therefore the entire liver is enlarged and the surface of the biopsy contains less hepatocytes than a similar sized biopsy of healthy liver tissue. To assess the relative amount of MAC387 or CD3 positive cells a cell count of hepatocytes could have been performed. No staining for neutrophils has been performed during this study, probably if this had been included the findings of the pathologist would have been confirmed. Another explanation could be, as mentioned before, hepatic lipidosis samples included are all taken in early stage of the disease, when the inflammatory and regenerative responses have not started yet.

Histological evaluation indicated eleven out of twelve diseased samples were negative for fibrosis, only one sample scored mildly positive for fibrosis. Hepatic stellate cells were activated in all feline lipidosis samples. HSCs are the first cells in the fibrogenic pathway and therefore fibrosis could be present, contradictory to the earlier histological evaluation. Sirius red staining demonstrated presence of fibrosis in all samples. Our results using the sirius red and αSMA staining for young collagen and fibrosis, demonstrate that fibrosis marker sirius red is increased in all samples. It seems that subsequent progression to fibrosis might be present during feline lipidosis but it is not properly evaluated with conventional histological staining.

To determine what role different cells have during feline hepatic lipidosis, further research is required, including additional markers for NK cells, neutrophils, IFN-γ and regeneration markers. To determine cells that are in cell cycle arrest staining for P21 has been suggested. Staining for P21 has been performed during this study but has not yet been optimized and therefore results are not included. Dissimilar between feline lipidosis and human medicine is that the presence of inflammation and fibrosis during NAFLD is generally thought to be a marker of poor prognosis. Looking at our results, the only cat that survived lipidosis, as far as we know from the history, had a marked increase in inflammation, fibrosis and little activation of hepatocyte proliferation. Obviously only one case is not enough to draw any conclusion but it would be interesting to relate IHC scoring to survival rates in cats with liver disease, namely lipidosis. In this study it is not possible to establish correlation between history, histological and immunoistochemistry score and prognosis. In fact for the majority of the cats which biopsies we evaluated, the history was fragmentary and often unavailable.

A liver biopsy displays only a small segment of the entire liver. During this study we encountered few problems that obstruct the ability to perform an adequate evaluation of all the samples of the liver biopsies. In fact histological evaluation of true cut biopsy samples

resulted to be quite difficult because of the small size and the possibility of strangely cut areas. True cut biopsies used are approximately between one and a half and five times smaller than wedge biopsies. Some samples did not contain a portal area or a central vein which made difficult to determine the histological location of cells and abnormalities. True cut biopsies contain less cells of interest compared to the wedge biopsies. Inclusion of portal areas and central veins is important but a minimal biopsy size or minimal amount of portal triads has not been determined[33,34]. In this study the number of portal triads has not been determined, this could be of interest for further research. The dissimilarities between biopsies could be due to the biopsy type but it could also be due to the fact that these biopsies have the highest NAS score. The control samples, true cut biopsies, contain more cells of interest compared to group 1. A study by Cole et al 2002 compared true cut and wedge biopsies diagnosing different liver conditions of 124 dogs and cats. In 65 out of 124 specimens diagnosis derived from true cut biopsies differed from the wedge biopsy diagnosis. Inadequate tissue representation with true cut biopsies may restrict pathological evaluation[34]. Another study including 264 patients with morbid obesity concluded true cut biopsies are as effective as wedge biopsies for determination of the steatosis degree[33]. Steatosis is a disease diffusely spread through the liver, for other liver diseases and parameters this finding may not apply. Only a very small part of the liver has been biopsied with the true cut biopsies and that part may not represent all parameters of the disease. To determine the exact location and severity of alterations in the liver, larger tissue samples are needed or multiple samples from different locations are desirable. Ideally, to better evaluate the progression of fibrosis, regeneration and inflammation in lipidosis in cats, these animals should be followed during the initial development, progression and eventually recover from the disease. To be able to do so we should consider to take a liver biopsy before the onset of lipidosis and multiple biopsies during the progression of the disease. The biopsies included in this study are in fact only snapshots at an unknown time point after the onset of disease; it was not reported in every patient when the clinical signs had started nor if the cat had been treated initially for the underlying disease. Unfortunately performing such a study would be considered by the majority as unethical, as lipidosis should be induced in research animals and liver biopsies performed at different time point. If we consider using client owned cats, we need to remember that cats with hepatic lipidosis are severely ill and need immediate medical care to be able to survive. Since their liver function is severely impaired and they often suffer from coagulopathy, exposing these cats to repeated anaesthesia and liver biopsies is unjustifiable and life threatening. A major drawback of using existing tissue samples however is lack of similarity between patient's clinical signs, underlying disease, treatment received, biopsies and time frame of when the biopsies were performed. Samples

used in this study are all from patients visiting the veterinarian or post-mortem examination of deceased cats. Age of cats included is another uncertainty. Age varies from a few months to ten years. Older cats may have encountered other liver related problems earlier in life and collagen depositions we see with sirius red might in fact be fibrosis that already existed before onset of lipidosis. During this study no relationship between age and fibrosis score has been found.

Conclusion.

Some changes in cats with lipidosis are similar to NAFLD in humans, such as increased myofibroblast activity and fibrotic depositions. However all changes in cats are mild compared to human lipidosis. Other aspects of NASH have not been demonstrated convincingly during the current study. Hepatocyte regeneration and the LPC compartment are usually not activated in feline lipidotic liver but one of them is always activated in other species with lipidosis. Inflammatory responses appear to be mildly present and contain mostly neutrophils which is different from human NAFLD. In conclusion the results in this study do not confirm our hypothesis on development of NAFLD, similar to humans, in cats with lipidosis.

References

1. Center SA. Feline hepatic lipidosis. *Vet Clin North Am Small Anim Pract*. 2005;35(1):225-269. doi: 10.1016/j.cvsm.2004.10.002.

2. Paschos P, Paletas K. Non alcoholic fatty liver disease and metabolic syndrome. *Hippokratia*. 2009;13(1):9-19.

3. Lewis JR, Mohanty SR. Nonalcoholic fatty liver disease: A review and update. *Dig Dis Sci*. 2010;55(3):560-578. doi: 10.1007/s10620-009-1081-0; 10.1007/s10620-009-1081-0.

4. Kleiner DE, Brunt EM, Van Natta M, et al. Design and validation of a histological scoring system for nonalcoholic fatty liver disease. *Hepatology*. 2005;41(6):1313-1321. doi: 10.1002/hep.20701.

5. Brunt EM, Kleiner DE, Wilson LA, Belt P, Neuschwander-Tetri BA, NASH Clinical Research Network (CRN). Nonalcoholic fatty liver disease (NAFLD) activity score and the histopathologic diagnosis in NAFLD: Distinct clinicopathologic meanings. *Hepatology*. 2011;53(3):810-820. doi: 10.1002/hep.24127; 10.1002/hep.24127.

6. Center SA, Guida L, Zanelli MJ, Dougherty E, Cummings J, King J. Ultrastructural hepatocellular features associated with severe hepatic lipidosis in cats. *Am J Vet Res*. 1993;54(5):724-731.

7. Takeishi T, Hirano K, Kobayashi T, Hasegawa G, Hatakeyama K, Naito M. The role of kupffer cells in liver regeneration. *Arch Histol Cytol*. 1999;62(5):413-422.

8. Fausto N, Campbell JS, Riehle KJ. Liver regeneration. *J Hepatol*. 2012;57(3):692-694. doi: 10.1016/j.jhep.2012.04.016; 10.1016/j.jhep.2012.04.016.

9. Kuramitsu K, Sverdlov DY, Liu SB, et al. Failure of fibrotic liver regeneration in mice is linked to a severe fibrogenic response driven by hepatic progenitor cell activation. *Am J Pathol*. 2013;183(1):182-194. doi: 10.1016/j.ajpath.2013.03.018; 10.1016/j.ajpath.2013.03.018.

10. Overturf K, al-Dhalimy M, Ou CN, Finegold M, Grompe M. Serial transplantation reveals the stem-cell-like regenerative potential of adult mouse hepatocytes. *Am J Pathol*. 1997;151(5):1273-1280.

11. Alison M. Liver stem cells: A two compartment system. *Curr Opin Cell Biol*. 1998;10(6):710-715.

12. Roskams T, Yang SQ, Koteish A, et al. Oxidative stress and oval cell accumulation in mice and humans with alcoholic and nonalcoholic fatty liver disease. *Am J Pathol*. 2003;163(4):1301-1311. doi: 10.1016/S0002-9440(10)63489-X.

13. Jaeschke H. Mechanisms of liver injury. II. mechanisms of neutrophil-induced liver cell injury during hepatic ischemia-reperfusion and other acute inflammatory conditions. *Am J Physiol Gastrointest Liver Physiol*. 2006;290(6):G1083-8. doi: 10.1152/ajpgi.00568.2005.

14. Naito M, Hasegawa G, Ebe Y, Yamamoto T. Differentiation and function of kupffer cells. *Med Electron Microsc*. 2004;37(1):16-28. doi: 10.1007/s00795-003-0228-x.

15. Viebahn CS, Yeoh GC. What fires prometheus? the link between inflammation and regeneration following chronic liver injury. *Int J Biochem Cell Biol*. 2008;40(5):855-873. doi: 10.1016/j.biocel.2007.11.025; 10.1016/j.biocel.2007.11.025.

16. Lee UE, Friedman SL. Mechanisms of hepatic fibrogenesis. *Best Pract Res Clin Gastroenterol*. 2011;25(2):195-206. doi: 10.1016/j.bpg.2011.02.005; 10.1016/j.bpg.2011.02.005.

17. Bataller R, Brenner DA. Liver fibrosis. *J Clin Invest*. 2005;115(2):209-218. doi: 10.1172/JCI24282.

18. Lemoinne S, Cadoret A, El Mourabit H, Thabut D, Housset C. Origins and functions of liver myofibroblasts. *Biochim Biophys Acta*. 2013;1832(7):948-954. doi: 10.1016/j.bbadis.2013.02.019; 10.1016/j.bbadis.2013.02.019.

19. Buckwalow IB, Böcker W. *Immunohistochemistry: Basics and methods.* Berlin: Springer Berlin Heidelberg; 2010.

20. Boenisch T, Taylor CR, Happel JF. *Education guide. DAKO IHC staining methods.* Vol 1. 5th ed. carpinteria: Dako north america; 2009.

21. Kamohara Y, Haraguchi N, Mimori K, et al. The search for cancer stem cells in hepatocellular carcinoma. *Surgery*. 2008;144(2):119-124. doi: 10.1016/j.surg.2008.04.008; 10.1016/j.surg.2008.04.008.

22. Strnad P, Paschke S, Jang KH, Ku NO. Keratins: Markers and modulators of liver disease. *Curr Opin Gastroenterol*. 2012;28(3):209-216. doi: 10.1097/MOG.0b013e3283525cb8; 10.1097/MOG.0b013e3283525cb8.

23. Scholzen T, Gerdes J. The ki-67 protein: From the known and the unknown. *J Cell Physiol*. 2000;182(3):311-322. doi: 2-9.

24. Parola M, Marra F, Pinzani M. Myofibroblast – like cells and liver fibrogenesis: Emerging concepts in a rapidly moving scenario. *Mol Aspects Med*. 2008;29(1–2):58-66. doi: 10.1016/j.mam.2007.09.002.

25. Junqueira LC, Bignolas G, Brentani RR. Picrosirius staining plus polarization microscopy, a specific method for collagen detection in tissue sections. *Histochem J*. 1979;11(4):447-455.

26. Veidal SS, Karsdal MA, Vassiliadis E, et al. MMP mediated degradation of type VI collagen is highly associated with liver fibrosis--identification and validation of a novel biochemical marker assay. *PLoS One*. 2011;6(9):e24753. doi: 10.1371/journal.pone.0024753; 10.1371/journal.pone.0024753.

27. Yang S, Koteish A, Lin H, et al. Oval cells compensate for damage and replicative senescence of mature hepatocytes in mice with fatty liver disease. *Hepatology*. 2004;39(2):403-411. doi: 10.1002/hep.20082.

28. Sydor S, Gu Y, Schlattjan M, et al. Steatosis does not impair liver regeneration after partial hepatectomy. *Lab Invest*. 2013;93(1):20-30. doi: 10.1038/labinvest.2012.142; 10.1038/labinvest.2012.142.

29. Katoonizadeh A, Nevens F, Verslype C, Pirenne J, Roskams T. Liver regeneration in acute severe liver impairment: A clinicopathological correlation study. *Liver Int*. 2006;26(10):1225-1233. doi: 10.1111/j.1478-3231.2006.01377.x.

30. Brunt EM, Janney CG, Di Bisceglie AM, Neuschwander-Tetri BA, Bacon BR. Nonalcoholic steatohepatitis: A proposal for grading and staging the histological lesions. *Am J Gastroenterol*. 1999;94(9):2467-2474. doi: 10.1111/j.1572-0241.1999.01377.x.

31. Sun R, Gao B. Negative regulation of liver regeneration by innate immunity (natural killer cells/interferon-gamma). *Gastroenterology*. 2004;127(5):1525-1539.

32. Strick-Marchand H, Masse GX, Weiss MC, Di Santo JP. Lymphocytes support oval cell-dependent liver regeneration. *J Immunol*. 2008;181(4):2764-2771.

33. Padoin AV, Mottin CC, Moretto M, et al. A comparison of wedge and needle hepatic biopsy in open bariatric surgery. *Obes Surg*. 2006;16(2):178-182. doi: 10.1381/096089206775565159.

34. Cole TL, Center SA, Flood SN, et al. Diagnostic comparison of needle and wedge biopsy specimens of the liver in dogs and cats. *J Am Vet Med Assoc*. 2002;220(10):1483-1490.

Appendix 1. Protocol K19

Two step IHC protocol cat: Keratin 19

1. Deparaffinise and rehydrate sections in a series of:
   Xylene: 2x5'; Alc. 96%; Alc. 80%; Alc. 70%; Alc. 60% (each step 5'); MQ 5'
2. Proteinase-K (Dako) 15 min. RT
3. Rinse in TBS/T buffer solution 2 x 2 min.
4. Inhibit endogenous peroxidise activity by incubating the slides in 'Dako Dual Endogenous Enzyme Block' 10 min. RT
5. Rinse in TBS/T buffer solution 3 x 5 min.
6. Incubate in 10 percent normal goat serum 30 min. RT
7. Incubate with (in ab-diluent, DAKO) 60 min. RT
   - K19 - #29 - 1:100 (mouse)
8. Rinse the sections in TBS/T buffer solution 3 x 5 min.
9. Incubate in 45 min. RT
   - Envision Goat anti mouse HRP
10. Rinse the sections in TBS (NO TWEEN) 3 x 5 min.
11. Incubate the sections in freshly made DAB substrate (Result: brown) 5 min.
12. Rinse the sections in mQ 3 x 5 min.
13. Counterstain the sections haematoxylin QS-Dako 10 sec.
14. Rinse sections in running tapwater 10 min.
15. Dehydrate section and cover in vectamount:
    5' 60% Alc; 5' 70% Alc; 5' 80% Alc; 5'96% Alc; 5'96% Alc; 2x 3' Xyleen

Buffers:

TBS/T: 100 ml of 10xTBS in 900ml mQ + 1 ml Tween.

Appendix 2. Protocol Ki67

Two step IHC protocol Ki67

1. Deparaffinize and rehydrate sections in a series of:
   Xylene: 2x5' ; Alc. 96%; Alc. 80% ; Alc. 70%; Alc. 60%; Alc. 30% (each step 5'); MQ 5'
2. Antigen retrieval in 10 mM hot citrate buffer pH 6.0 — 30 min. 98°C
   (3.36 gr in 1600 ml mQ, adjust pH to 6)
   Cool down at room temperature (still in hot buffer outside water bath) — 30 min.
3. Rinse in PBS/T buffer solution — 2 x 2 min.
4. Inhibit endogenous peroxidase activity by incubating the slides in — 10 min. RT
   Dako Ready to use peroxidase block
5. Rinse in PBS/T buffer solution — 3 x 5 min.
6. Incubate in 10 percent normal goat serum/PBS — 30 min. RT
7. Incubate with (in ab-diluent, DAKO) — O/N at 4°C
   - Ki67 #115 (MIB-1) fridge ; 1:50
8. Rinse the sections in PBS/T buffer solution — 3 x 5 min.
9. Incubate in
   - Envision Goat anti mouse HRP — 45 min. RT
10. Rinse the sections in PBS — 3 x 5 min.
11. Incubate the sections in freshly made DAB substrate (result: brown) — 5 min.
12. Rinse the sections in mQ — 3 x 5 min.
13. Counterstain the sections haematoxylin QS-Dako — 10 sec.
14. Rinse sections in running tapwater — 10 min.
15. Dehydrate section and cover in vectamount:

3' 60% alcohol; 3' 70% alcohol; 3' 96% alcohol; 3' 96% alcohol; 3' 100% alcohol; 2x3' xyleen

Buffer: 10 mM Citrate buffer (pH 6.0) Add 2.1 gram citric acid to 1000 ml mQ Adjust pH with NaOH

Appendix 3. Protocol αSMA

Two step IHC protocol cat: αSMA

1.	Deparaffinise and rehydrate sections in a series of: Xylene: 2x5'; Alc. 96%; Alc. 80%; Alc. 70%; Alc. 60% (each step 5'); MQ 5	
2.	Block endogenous peroxidise activity in 1% H2O2 in methanol	30 min. RT
3.	Rinse in PBS/T Buffer solution	3 x 5 min.
4.	Incubate in 10 Percent normal goat serum in PBS	15 min. RT
5.	Incubate with mouse anti αSMA in PBS	
	a. αSMA #16 1:200 (Mouse)	60 min. RT
6.	Rinse the sections in PBS/T buffer solution	3 x 5 min.
7.	Incubate in:	
	a. Envision Goat anti mouse HRP	45 min. RT
8.	Rinse the sections in PBS	3 x 5 min.
9.	Incubate the sections in freshly made DAB substrate (result:Brown)	5 min.
10.	Rinse the sections in mQ	3 x 5 min.
11.	Counterstain the sections haematoxylin QS-Dako	10 sec.
12.	Rinse sections in running tapwater	10 min.
13.	Dehydrate section and cover in vectamount: 5' 60% Alc; 5' 70% Alc; 5' 80% Alc; 5'96% Alc; 5'96% Alc; 2x 3' Xyleen	

Buffers: 1% H2O2 in methanol: add 1,4 ml H2O2 (35%) to 50 ml of methanol.

Appendix 4. Protocol sirius red.

sirius red/ Haematoxylin staining

Picro-sirius red Solution

sirius red F3B (C.I. 35782) ---------- 0.5 g

Saturated aqueous solution of picric acid ---------500 ml

(Keeps for at least 3 years and can be used many times)

Acidified Water

Add 5 ml acetic acid (glacial) to 1 liter of water (tap or distilled)

1. Deparaffinize and rehydrate sections in series of:
   Xyleen 4min, Alc 100% 4min, Alc 96% 4min, Alc 70% 4min and mQ 4min.
2. Stain in picro-sirius red for one hour (This gives near-equilibrium staining, which does not increase with longer times. Shorter times should not be used, even if the colors look OK.)
3. Wash in two changes of acidified water.
4. Physically remove most of the water from the slides by vigorous shaking. Wash in Mq. (optional: draw with EmmEdge pen around tissue)
5. Incubate with Haematoxylin for 10sec
6. Wash the slides for 10 minutes in running tap water
7. Dehydrate in three changes of 100% ethanol: Alc 70% 3min, Alc 96% 3min, Alc 100% 3min,
   Xyleen 2x2min.
8. Cover in Vectamount

Appendix 5. Protocol MAC387.

Two step IHC protocol MAC387

1. Deparaffinise and rehydrate sections in a series of:
   Xylene: 2x5'; Alc. 96%; Alc. 80%; Alc. 70%; Alc. 60%; Alc. 30% (each step 5'); MQ 5'
2. Proteinase-K (Dako) 10 min. RT
3. Rinse in PBS/T Buffer solution 2 x 2 min.
4. Inhibit endogenous peroxidise activity by incubating the slides in 'Dako Dual Endogenous Enzyme Block' 10 min. RT
5. Rinse in PBS/T Buffer solution 3 x 5 min.
6. Incubate in 10 Percent normal goat serum in PBS 30 min. RT
7. Incubate with (in ab-diluent, DAKO)
   a. MAC387 – 37 – 1:1000 (mouse) O/N at 4°C
8. Rinse in PBS/T Buffer solution 3 x 5 min.
9. Incubate in
   a. Envision Goat anto mouse HRP 45 min. RT
10. Rinse the sections in PBS 3 x 5 min.
11. Incubate the sections in freshly made DAB substrate (result:Brown) 5 min.
12. Rinse the sections in mQ 3 x 5 min.
13. Counterstain the sections haematoxylin QS-Dako 10 sec.
14. Rinse sections in running tapwater 10 min.
15. Mount in Aquamount/Faramount (Dako) (= aquaeous, de geen dehydratiestappen nodig!)
    Or
    Dehydrate section and cover in vectamount:
    3' 30% Alc; 3' 70% Alc; 3' 96% Alc; 3'100% ; 2x 3' Xyleen

Appendix 6. Protocol CD3

Two step IHC protocol CD3

1. Deparaffinise and rehydrate sections in a series of:
   Xylene: 2x5'; Alc. 96%; Alc. 80%; Alc. 70%; Alc. 60%; Alc. 30% (each step 5'); MQ 5'
2. Antigen retrieval in hot citrate buffer(10 mM, pH 6,0) 30 min. 98°C
   Cool down at room temperature (still in hot buffer, outside the water bath) 30 min.
3. Rinse in PBS/T buffer solution
   2x2min.

16. Block endogenous peroxidise activity by incubating the slides in 10 min. RT
4. 'Dako Dual Endogenous Enzyme Block'
5. Rinse in PBS/T buffer solution
   3x5min. RT
6. Incubate in 10% normal goat serum in PBS to reduce background staining. 15 min. RT
7. Incubate with (In antibody diluent) 60 min. RT
   - primary antibody rabbit anti CD3 (Wedge biopsies 1:200)
   - primary antibody rabbit anti CD3 (FNAB 1:200)
8. Rinse sections in PBS/T 3x5 min.
9. Incubate in 45 min. RT
   - Envision goat anti rabbit HRP
10. Rinse in PBS buffer solution 3x5min.
11. Incubate sections is freshly made DAB substrate (Result: Brown) 5 min.
12. Rins in MQ 3x5 min.
13. Counterstain sections haematoxylin QS-Dako 1:1 10 sec
14. Rinse sections in running tap water 10 min
15. Dehydrate section and cover in vectamount:
    3' 30% alcohol; 3' 60% alcohol; 3' 70% alcohol; 3'80% alcohol; 3' 96% alcohol; 3' 100% alcohol; 2x3' Xylene

Appendix 7. Original scores K19

ID	Result K19 staining	Portal	periportal	parenchyma	NAS score
Group 1					
P9609378	Bile ducts stain positive with more K19 activity than usual and there are few positive cells just outside the portal area.	2	1	0	6
P0102523	There is no portal area included in this slide but there seems to be a periportal area and in the parenchyma there seems to be a ductular reaction.	0	2	2	6
P0110084	Bile ducts stain positive with more K19 activity than usual, periportal there are positive clusters of cells. *In parenchym moderate number of clusters positive cells (Ductular reaction)*	3	2	0	5
P0309444	Bile ducts stain positive with more activity than usual, periportal there is some k19 activity.	2	1	0	6
P0312037	Portal area contains more K19 positivity than usual. There appears to be activity outside the portal area and ductular reaction in the parenchyma but this is difficult to say due to the bad quality of the biopsy.	2	1	2	7
P0410061	No portal area included in this slide, no k19 positivity visible.	0	0	0	6
Group 2					

J310113000502	Portal and periportal there is increased K19 activity. Little positive cells visible in the parenchyma	2	2	1	5
J310082704402	In the parenchyma there is a clear ductular reaction, periportal there is high K19 activity and portal there is mildly increased K19 expression.	2	3	3	5
J311051000202	In the portal area the bileducts are stretched, no longer round. Periportal there is some k19 activity. In the parenchyma there is a ductular reaction.	1	1	2	5
Group 3					
J311061503102	Bile ducts stain positive, periportal and parenchymal there are clusters K19 positive cells	1	2	2	1
J311121504002	Portal and periportal area show mildly increased k19 expression.	2	2	1	3
J311031104902	K19 positivity is increased severely, a severe ductular reaction is present with portal bridging.	4	3	4	4
Control group					
Rafael	In the portal area the bile ducts are stretched, there is an increase in k19 positive loose cells periportal and parenchymal, this appears not a ductular reaction	3	2	1	0
Mazzel	There is increased K19 activity in the portal area and there seem to be some positive cells	2	0	1	0

	in the parenchyma.				
Ozzy	In the portal area the k19 activity is normal, periportal there are clusters of k19 positive cells.	1	2	0	0

Appendix 8. Original scores ki67.

ID	Ki67 results (Cells/five 40X fields)	NAS score
Group 1		
P9609378	4	6
P0102523	1	6
P0110084	0	5
P0309444	0	6
P0312037	1	7
P0410061	0	6
Group 2		
J310113000502	0	5
J310082704402	15 Clustered	5
J311051000202	3 Clustered	5
Group 3		
J311061503102	7 Clustered	1
J311121504002	1	3
J311031104902	32	4
Control group		
Rafael	3	0
Mazzel	5	0
Ozzy	11	0

Appendix 9. Original scores αSMA.

ID	Result αSMA description	portal	periportal	parenchyma	NAS score
Group 1					
P9609378	In the portal area αSMA positive vessels look as expected. Periportal there is a moderate increase in positive cells, as well as in the parenchyma.	1	3	2	6
P0102523	In the periportal area and parenchyma there is an increase in cells staining positive. αSMA positivity in the portal area is limited to endothelial cells.	1	2	2	6
P0110084	Endothelial cells in the portal area stain positive, periportal and parenchymal there is a mild increase in αSMA positive cells.	1	1	1	5
P0309444	In the portal area αSMA positivity is increased and peri portal there is an increase in positive cells as well. There is no αSMA expression in the parenchyma	3	2	0	6
P0312037	Only endothelial cells in portal area.	3	3	3	7
P0410061	Throughout the tissue there is some sort of orange-brown granular pigment present. Endothelial cells in the portal area stain positive and periportal there are also cells staining positive.	1	1	0	6
Group 2					
J310113000502	Mildly increased αSMA positivity in the portal area, moderate	2	2	4	5

	increase periportal and a strong increase in the parenchyma, mainly in the sinusoids.				
J310082704402	The portal areas look as expected, periportal however there is a moderate to severe increase in αSMA positivity, in the parenchyma there is a strong increase, mostly in the sinusoids.	1	3	4	5
J311051000202	αSMA positivity is mildly increased in the portal area and there is a strong increase in the periportal and parenchymal area. Positive cells find themselves mainly in the sinusoids.	2	4	4	5
Group 3					
J311061503102	In the portal area there is a mild increase in αSMA positive cells. Throughout the tissue, in parenchyma and periportal areas increased amounts of cells stain positive.	2	2	3	1
J311121504002	There is a mild to moderate increase in αSMA positivity throughout the tissue.	2	2	2	3
J311031104902	Throughout the tissue there is a strong increase in αSMA positivity.	4	4	4	4
Control group					
Rafael	The portal area stains as expected, periportal there is a slight increase in αSMA positivity and also in sinusoids the cell borders stain positive in several places. Possibly a stellate cell reaction, less probable they are	1	1	1	0

	weird cut portal areas.				
Mazzel	There is slightly more αSMA avtivity in the portal area than expected, as well as in the periportal and parenchymal area.	2	1	1	0
Ozzy	The portal area is as expected, there is a slight increase in αSMA activity in the periportal area.	1	1	0	0

Appendix 10. Original scores sirius red.

ID	Result sirius red(SR) staining	portal	periportal	parenchyma	NAS score
Group 1					
P9609378	The portal area stains as expected, periportally there is a mild increase in SR positive stripes, in the parenchyma these stripes can be found too in a small amount.	1	2	1	6
P0102523	There is a strong increase in SR positivity in the portal and periportal area. In the parenchyma moderate amounts of sr positive thin strings can be found.	3	3	2	6
P0110084	In the portal area there is a mild increase in SR positivity, periportal and parenchymal there is a slight increase in fine SR positive lines.	2	1	1	5
P0309444	The portal area is slightly more positive than expected, in the periportal area and parenchyma small amounts of positive strings can be found.	2	1	1	6
P0312037	The portal area has strongly increased SR positivity. From the portal area a moderate number of thin positive lines migrate into the surrounding tissue. In the parenchyma there are few thin positive lines.	4	3	1	7
P0410061	Portal and periportal there is a moderate increase in SR positive	3	3	2	6

	tissue, as well as in the parenchyma where the increase in mild to moderate.				
Group 2					
J310113000502	The portal area stains as expected, the periportal area has a slight increase in thin positive strings. In the parenchyma no positivity has been found.	1	1	0	5
J310082704402	There is a mild increase in portal positivity and a mild to moderate increase in positive thin lines in the periportal and parenchymal area.	2	2	2	5
J311051000202	The portal area looks as expected, there is a slight increase in small SR positive strings through the surrounding tissue.	1	1	1	5
Group 3					
J311061503102	The portal area is as expected, periportally and parenchymal little positive thin Red strings can be seen.	1	1	1	1
J311121504002	In the portal area positivity has moderately increased, periportal there are thin positive lines. In the parenchyma no positivity could be found.	3	1	0	3
J311031104902	The portal area looks as expected when normal, periportal there are little thin red lines visible. In the parenchyma there is a moderate to severe increase in SR positivity in a portal bridging pattern but in between	1	1	3	4

	there are mild amounts of positive line visible.				
Control group					
Rafael	In the portal area staining has moderate to severely increased, periportal there is a moderate increase and in the parenchyma there are some positive red lines visible.	3	2	1	0
Mazzel	The portal area stains slightly positive, this is probably normal in the catliver. Periportal no positivity has been discovered. In the parenchyma however little positive thin lines can be seen between the hepatocytes.	1	0	1	0
Ozzy	The portal area stains slightly positive, this is probably normal in the catliver. Periportally there is a slight increase in positive thin lines between the cells. In the parenchyma no positivity has been seen.	1	1	0	0

Appendix 11. Original scores MAC387.

ID	Results MAC	portal	periportal	parenchymal	NAS score
Group 1					
P9609378	Positive cells are spread all over the tissue in a mild amount.	1	1	1	6
P0102523	Positive cells are mainly located throughout the parenchyma in a mild to moderate amount.	0	0	2	6
P0110084	Positive cells are all over the tissue in a mild amount.	1	1	1	5
P0309444	There are no positive cells in the portal areal but they are present in the periportal and parenchymal area in a mild amount.	0	1	1	6
P0312037	Only in the parenchymal area positive cells can be found in a mild amount.	0	0	1	7
P0410061	Positive cells can be found throughout the entire tissue in a mild amount.	1	1	1	6
Group 2					
J310113000502	There is a severe increase of positive cells in the vessels in the portal area. There is a moderate to severe amount of positive cells that have spread through the rest of the tissue	4	3	3	5
J310082704402	There are little positive cells in the portal area, there is a moderate increase of positive cells in the periportal area and a mild to moderate increase in the parenchyma	1	3	2	5
J311051000202	Throughout the tissue a mild amount of cells are present	1	1	1	5
Group 3					
J31106150	There is a slightly increased number of	2	1	1	1

3102	positive cells in the portal area and a mild amount through the rest of the tissue				
J311121504002	The number of positive cells is increased portally and periportally and there is a mild amount of positive cells in the parenchyma	2	2	1	3
J311031104902	There is a moderate to severe increase in the portal area and a severe amount of positive cells in the periportal and parenchymal area.	3	4	4	4
Control group					
Rafael	Throuthout the tissue there is a mild to moderate amount of positive cells present.	2	2	2	0
Mazzel	Positive cells are mainly situated in the portal area and in the parenchyma. There is a mild amount of cells in the periportal area.	2	1	2	0
Ozzy	Positive cells are mainly situated in the periportal area, throughout the tissue a small amount of positive cells can be seen.	1	2	1	0

Appendix 12. Scores inflammatory cells

ID	CD3 results (Cells/five 40 X fields)	MAC387 Cell count/surface	NAS score
Group 1			
P9609378	0	112/43430	6
P0102523	3	17/10468	6
P0110084	0	28/35879	5
P0309444	0	66/23135	6
P0312037	3	21/16316	7
P0410061	0	56/14517	6
Group 2			
J310113000502	2	332/55619	5
J310082704402	15	142/55569	5
J311051000202	35 Mainly parenchymal	224/55687	5
Group 3			
J311061503102	7	182/44794	1
J311121504002	7	175/55212	3
J311031104902	28 Mainly portal	2287/53365	4
Control group			
Rafael	9	344/31655	0
Mazzel	4	118/24599	0
Ozzy	8	83/27796	0